Label-free Biosensing Based on Single Gold Nanostars as Plasmonic Transducers

Srujan K. Dondapati,[†] Tapan K. Sau,[†] Calin Hrelescu,[†] Thomas A. Klar,[‡] Fernando D. Stefani,[†,‡,]* and Jochen Feldmann[†]

[†]Photonics and Optoelectronics Group, Physics Department and Center for Nanoscience (CeNS), Ludwig-Maximilians-Universität München, Amalienstrasse 54, 80799 Munich, Germany, and [‡]Institute of Physics and Institute of Micro- and Nanotechnologies, Technical University of Ilmenau, 98684 Ilmenau, Germany. [§]Present address: Departamento de Física & Instituto de Física de Buenos Aires (IFIBA, CONICET), Facultad de Ciencias Exactas y Naturales, Universidad de Buenos Aires, Ciudad Universitaria (1428) Buenos Aires, Argentina.

ABSTRACT Gold nanostars provide high sensitivity for single nanoparticle label-free biosensing. The nanostars present multiple plasmon resonances of which the lower energy ones, corresponding to the nanostar tips and core—tip interactions, are the most sensitive to environmental changes. Streptavidin molecules are detected upon binding to individual, biotin-modified gold nanostars by spectral shifts in the plasmon resonances. Concentrations as low as 0.1 nM produce a shift of the tip related plasmon resonances of about 2.3 nm (5.3 meV).

N oble metal nanoparticles have found wide applications in bioanalytic[1] as well as photonic applications owing to their unique light scattering and absorption properties.[2,3] These properties arise from resonant oscillations of the conducting electrons of the nanoparticles called localized surface plasmon resonances (LSPRs). The energies of LSPRs lie typically in the optical regime and depend on the nanoparticle size, shape, and composition as well as on the orientation of the electric field relative to the particle and the dielectric properties of the surrounding medium.[4,5] The latter dependence of the LSPRs on the nanoparticle surroundings has been exploited to realize a number of label-free biosensors.[6—14] Persistent efforts have been made to finely tune the composition, shape, and size of metallic nanoparticles and thereby control their optical properties. Recently, a new kind of metallic nanoparticle, called nanostars has been synthesized.[15] The nanostars are composed of a central core from which a number of protruding tips extend. They typically show a LSPR of the core and multiple LSPRs corresponding to the tips and core—tip interactions. The latter are polarization dependent and accompanied by large local electric field enhancements at the sharp ends of

*Address correspondence to
fernando.stefani@df.uba.ar.

the tips.[16] Those locally enhanced fields have been exploited to amplify Raman signals (surface-enhanced Raman spectroscopy, SERS) allowing molecular detection at zeptomolar levels[17] and, very recently, have enabled the demonstration of SERS at the single gold nanostar level.[18] As a consequence of the confined electric field enhancement at the tips, the spectral positions of the LSPRs of a nanostar are expected to depend strongly on the dielectric environment around the tips. In this paper, we characterize this dependency at the single nanoparticle level and demonstrate its application for the detection of biomolecular interactions using the well-known streptavidin—biotin assay.

RESULTS AND DISCUSSION

Single gold nanostars were located and investigated spectroscopically in a dark-field microscope equipped with a spectrometer coupled to a liquid-nitrogen cooled, back illuminated CCD camera. The nanostars present multiple LSPRs. A representative polarization dependent scattering spectrum of a single nanostar is shown in Figure 1C. Multipeak (Lorentzian) fits to these spectra reveal the presence of four resonances. Although the nanostars may present more observable resonances, for consistency we focused our single-particle investigations on nanostars whose spectra could be satisfactorily fitted with four resonances exclusively.

Figure 1D shows a scatter plot of the amplitude *vs* position obtained from 4-Lorenzain fits to the polarization dependent spectra of Figure 1C and is representative of all nanostars investigated. In all cases we observe the nanostars present one weak and nearly polarization-independent resonance
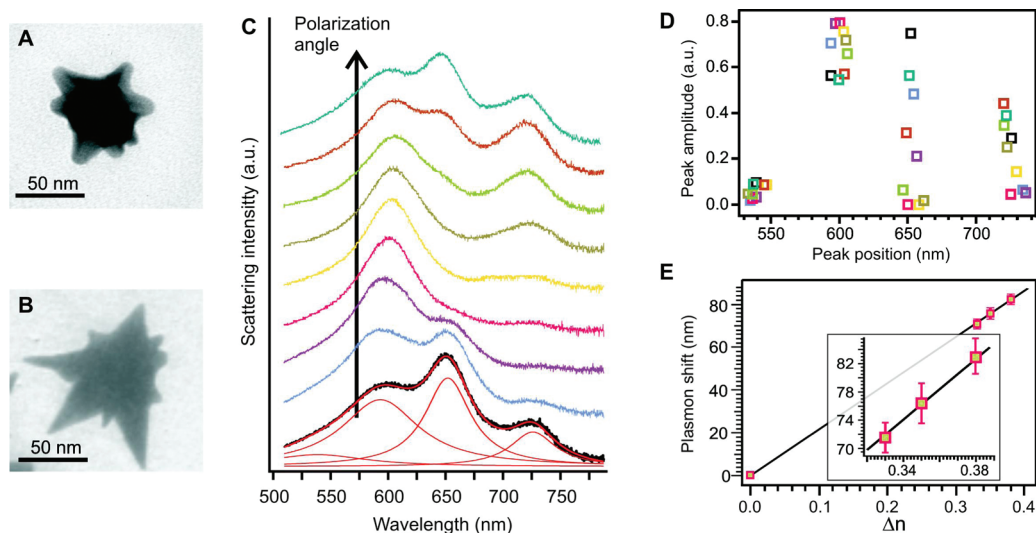
Figure 1. Structure and scattering of gold nanostars. (A and B) transmission electron microscopy (TEM) images of two gold nanostars. (C) Polarized light scattering spectra of a single gold nanostar immobilized on a glass substrate (in 0.1 M PBS buffer solution; pH 6.8) as a function of the polarization angle (0°−180°) of the incident light. The spectra are vertically offset for clarity. A four-peak (Lorenzian) fit to the first spectrum is shown. (D) Scatter plot of the amplitude vs position obtained from 4-Lorenzian fits to the spectra shown in panel C. (E) Average spectral shift of nanostars resonances peaking between 650 and 750 nm as a function of the surrounding refractive index. Data points for air ($n = 1.00$), Millipore water ($n = 1.33$), and 0.35 and 0.95 M glucose water solutions ($n = 1.35$ and $n = 1.38$, respectively).

at around 540−560 nm which we ascribe to the nanostar core. The longer wavelength resonances are polarization dependent and are attributed to the tips or the interaction between tips and core.[16] We note the peak at around 610 nm presents a weaker polarization dependency than expected for a tip or core−tip interaction resonance. A possible explanation is the spectral superposition of tip or tip−core resonances corresponding to similar, but differently oriented tips.

To test the magnitude of the spectral shift of the LSPRs upon bulk changes in the refractive index, we measured the spectra of individual nanostars in air, water (Milli Q), and glucose solutions of different concentrations (Figure 1D). We quantify the shift of each peak with a four-peak (Lorentzian) fit to each spectrum. Since the spectral position of the resonances varies from one nanostar to another, in order to characterize the typical behavior of the nanostars, we computed the average response of resonances from different nanostars peaking between 650 and 750 nm. The determined average sensitivity is 218 nm/RIU (Figure 1D). Considering the average fwhm of 43 nm for the resonances computed, we obtain a figure of merit (FOM) for the sensitivity of 5, which is within the range of FOM values reported for Au nanostars,[15] above Au bipyramids[19] and much higher than other Au nanomorphologies (0.6 for spheres, 1.5 for nanocubes, 2.6 for nanorods).[19] Figure 2 shows a schematic of the assay. The biotinylated gold nanostars provide a number of binding sites for streptavidin (SA).

Figure 3A shows the scattering spectra of a single biotin-functionalized gold nanostar before and after incubation with a 1 μm streptavidin (SA) solution (in 0.1 M PBS buffer solution; pH =

6.8). When SA binds to the biotin moieties on the nanostar surface, the plasmon resonances shift to lower energies (longer wavelengths) due to the increase in local refractive index.[8,14,20] Again in this case we quantified the plasmon shifts with a four-peak (Lorentzian) fit to the spectra of the single nanostars (Figure 3A). The peak labeled as "0" attributed to the plasmon of the nanostar core, is polarization independent and shows the smallest response to SA. We focused on the more sensitive longer wavelength resonances. In this case we quantify the shift in wavelength units (Figure 3A) and observe an unambiguous trend. The longer wavelength (lower energy) peaks respond to the presence of SA target molecules with a stronger shift (Figure 3B) in agreement with the previous reports and theoretical calculations.[14,21−23] A larger detectable wavelength shift is of valuable practical advantage for biosensing purposes. In addition, we observe the same trend for the relative spectral shift: $\Delta\lambda/\lambda \approx \Delta E/E = 1.10\%$, 1.11%, and 1.36% for peaks 1, 2, and 3, respectively, which indicates the lower energy resonances are fundamentally more sensitive to dielectric changes of the environment.[24]

The specificity of the biotinylated-nanostars was tested in a series of control experiments where again we considered the lowest energy resonance of
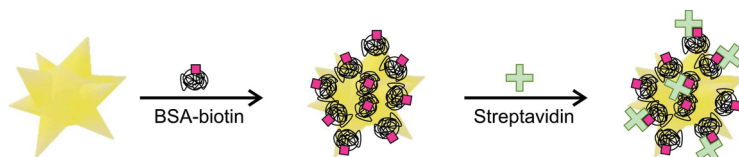

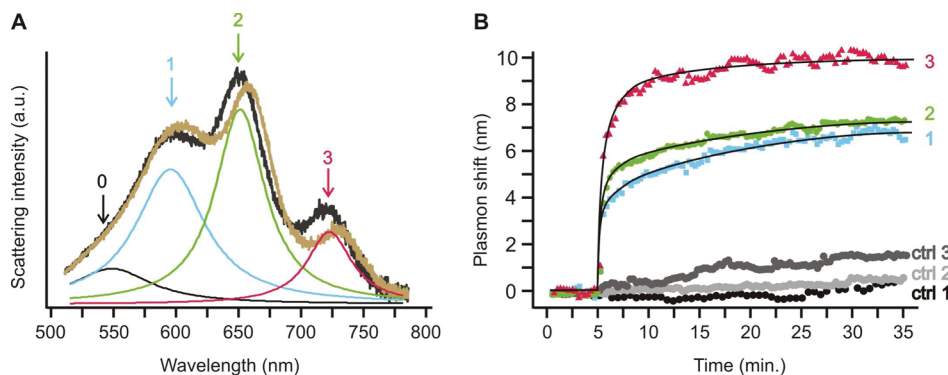Figure 2. Schematic representation of streptavidin−biotin interactions on a single gold nanostar.

Figure 3. (A) Scattering spectra of a single gold nanostar before (black) and 30 min after the incubation in a 1 μm SA solution (brown). The curves are the Lorentzian peaks obtained from the fit to the spectra before incubation with SA. **(B)** Time-dependent plasmon peak shifts corresponding to the three peaks of the biotin-modified gold nanostar shown in A for 1 μm streptavidin concentration. Typical control curves obtained for nanostars resonances peaking between 650 and 750 nm: (ctrl 1) pure buffer, (ctrl 2) addition of 1 μm BSA, (ctrl 3) response of a gold nanostar modified with nonbiotinylated BSA to a 1 μm streptavidin solution.

nanostars lying in the 650−750 nm range. Typical control curves are shown in Figure 3B. First, we controlled the stability of the LSPRs in the buffer solution. No shifts are observed (ctrl 1). Second, we tested the nanostars response to 1 μm BSA solution. BSA has a molecular weight similar to SA and thus the SA and BSA solutions have comparable refractive indices. Only a very small shift is observed at long incubation times due to unspecific binding (ctrl 2). Finally, we performed an additional control measurement with gold nanostars modified with nonbiotinylated BSA. In this case, there is an LSPR shift of around 1.5 nm due to the nonspecific adsorption of streptavidin (ctrl 3).

We analyzed in detail the response of the different plasmon resonances as a function of the polarization angle of the incident light. The scattering spectra of individual nanostars were acquired for different polarization angles (as in the example shown in Figure 1) before and after the addition of SA. Figure 4A shows the shift of the plasmon resonances labeled as "0", "1", "2", and "3" in Figure 3A as a function of the polarization angle, before and after the addition of 1 μm SA. The shift produced upon addition of SA is fairly independent of polarization. In Figure 4B, the plasmon shifts produced on 21 resonances of six different nanostars after incuba-

tion with 1 μm SA are shown as a function of the spectral position of the resonances. As expected,[14,21−23] longer wavelength plasmon resonances present a larger shift.

Finally we characterize the sensitivity of the single nanostar assay for different concentrations of the target molecule. Figure 5A shows the real-time monitoring of the shift of plasmon resonances of single biotinylated nanostars incubated in different concentrations of SA. In each case we consider the longest wavelength resonance, which were all between 680 and 740 nm. Upon pipetting of 1 μm streptavidin to the system after 5 min, there is a drastic red shift of the plasmon peak within 2 min, reaching a saturation limit of about 10 nm. Lower concentrations require more time to produce smaller shifts: for 0.1 μm, 10 nM, and 1 nM, there is a steady state plasmon shift of around 8, 6.5, and 4.2 nm. For the lower concentrations, a clear saturation is not observed even after 30 min.

The average plasmon shifts taken from five different nanostars as a function of the SA are shown in Figure 5B. The nanostars are highly sensitive to the presence of analyte leading to a very limited linear-response range (<1 nM). The smallest concentration that we
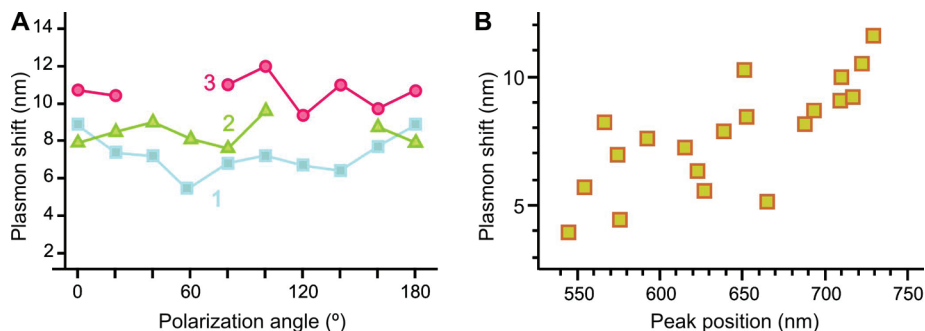

Figure 4. (A) Shift of the plasmon resonances of the biotinylated gold nanostar whose spectrum is shown in Figure 3 as a function of the angular position of the polarization analyzer upon incubation with 1 μm SA. The missing points correspond to polarizations where the LSPRs are not excited and thus no fit could be performed. **(B)** Plasmon shifts produced by 1 μm SA on the resonances of biotinylated nanostars as a function of the spectral position of the resonances.
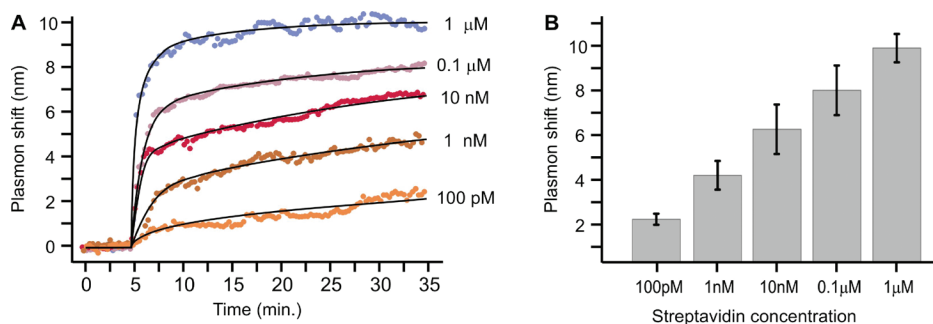
Figure 5. (A) Real time measurements of the plasmon peak shift of the LSPR "3" of single biotin-modified gold nanostar for different streptavidin concentrations. (B) Average shifts as a function of the SA concentration (five different nanostars for each concentration). The error bars indicate plus−minus a standard deviation. The line is a guide to the eye.

could detect reliably was 100 pM for which a clear plasmon shift of around 2.3 nm was observed.

CONCLUSIONS

We have investigated the performance of single gold nanostars as plasmonic transducers for label-free biosensing, by using the well-established biotin-SA assay. We analyzed spectroscopically and as a function of polarization the response of individual nanostars to molecular binding. We find that longer wavelength (lower energy) plasmon resonances present a larger response. Although the spectra of single nanostars depend strongly on relative orientation of the nanoparticle and light polarization, the shift produced on a particular resonance upon molecular binding is fairly polarization independent. Concentrations as low as 100 pM could be detected by a plasmon shift of 2.3 nm. We attribute this high sensitivity to (i) high sensitivity of the nanostar plasmon resonances to the local environment, (ii) more efficient binding of SA due to the hyper-branched structure of the nanostars, or a combination of both i and ii. Future experiments should focus on the concentration dependence of the sensor signal and a quantification of the number of SA molecules binding per gold nanostar.

METHODS

Biotin-Functionalized Nanostars. Gold nanostars were prepared in a one-pot synthesis in aqueous solution using cetyltrimethyl-ammoniumbromide (CTAB) as capping agent following a published method.[18] CTAB was partly replaced with biotinylated bovine serum albumin (BSA) by the following procedure. A sample of the original gold nanostar colloid is diluted 1:100 in pure water (Milli Q system, Millipore) and centrifuged at 3000 rpm (rotor diameter 12 cm) for 5 min. Then, 90% of the supernatant is removed and replaced with a water solution of 0.5% biotinylated BSA (Sigma). The centrifugation is performed one more time; the pellet is removed and replaced with water.

Characterization of the Biotinylated Nanostars. The size and shape of the biotinylated nanostars were characterized by transmission electron microscopy (TEM). Two TEM images of typical nanostars are shown in Figure 1A,B. The nanostars have a core size ranging from 30 to 50 nm and different number of conical tips with lengths varying from 10 to 60 nm.

For the optical spectroscopy investigation the nanostars were immobilized on glass coverslips that were first cleaned by sonication in isopropyl alcohol, then rinsed with isopropyl alcohol and sonicated in 1% HellmanexII detergent solution. After rinsing in water the substrates were further sonicated in Milli Q water and dried with N_2 gas. Then polyethyleneimine (PEI) was spin-coated (1 mg/mL, 3000 rpm) to provide a positively charged surface suitable for the electrostatic immobilization of the biotinylated gold nanostars. The so-prepared coverslips were incubated in a solution of nanostars and then thoroughly rinsed with distilled water. The nanostar concentration and incubation time were adjusted to obtain a surface density of less than one nanostar per squared micrometer which is suitable for the single nanostar measurements in the optical microscope.

REFERENCES AND NOTES

1. Klar, T. A. In *Nanophotonics with Surface Plasmons*; Shalaev, V. M., Kawata, S., Eds.; Advances in Nano-optics and Nano-photonics; Elsevier: Amsterdam, The Netherlands, 2007.
2. Murray, W. A.; Barnes, W. L. Plasmonic Materials. *Adv. Mater.* **2007**, *19*, 3771–3782.
3. Kelly, K. L.; Coronado, E.; Zhao, L. L.; Schatz, G. C. The Optical Properties of Metal Nanoparticles: The Influence of Size, Shape, and Dielectric Environment. *J. Phys. Chem. B* **2003**, *107*, 668–677.
4. Sönnichsen, C.; Franzl, T.; Feldmann, J.; Wilk, T.; Wilson, O.; Mulvaney, P. Drastic Reduction of Plasmon Damping in Gold Nanorods. *Phys. Rev. Lett.* **2002**, *88*, 077402.
5. Nehl, C. L.; Hafner, J. H. Shape-Dependent Plasmon Resonances of Gold Nanoparticles. *J. Mater. Chem.* **2008**, *18*, 2415–2419.
6. Englebienne, P. Use of Colloidal Gold Surface Plasmon Resonance Peak Shift To Infer Affinity Constants from the Interactions between Protein Antigens and Antibodies Specific for Single or Multiple Epitopes. *Analyst* **1998**, *123*, 1599–603.
7. Nath, N.; Chilkoti, A. A. Colorimetric Gold Nanoparticle Sensor to Interrogate Biomolecular Interactions in Real Time on a Surface. *Anal. Chem.* **2002**, *74*, 504–509.
8. Raschke, G.; Kowarik, S.; Franzl, T.; Sönnichsen, C.; Klar, T. A.; Nichtl, A.; Kürzunger, K.; Feldmann, J. Biomolecular Recognition Based on Single Gold Nanoparticle Light Scattering. *Nano Lett.* **2003**, *3*, 935–938.
9. Mcfarland, A. D.; Duyne, R. P. Single Silver Nanoparticles as Real-Time Optical Sensors with Zeptomole Sensitivity. *Nano Lett.* **2003**, *3*, 1057–1062.
10. Baciu, C. L.; Becker, J.; Janshoff, A.; Sönnichsen, C. Protein−Membrane Interaction Probed by Single Plasmonic Nanoparticles. *Nano Lett.* **2008**, *8*, 1724–1728.

11. Hernandez, F. J.; Dondapati, S. K.; Ozalp, V. C.; Pinto, A.; Klar, T. A.; Katakis, I. Label-free Optical Sensor for Avidin Based on Single Gold Nanoparticles Functionalized with Aptamers. *J. Biophoton.* **2009**, *2*, 227–231.

12. Mayer, K. M.; Lee, S.; Liao, H.; Rostro, B. C.; Fuentes, A.; Scully, P. T.; Nehl, C. L.; Hafner, J. H. A Label-free Immunoassay Based upon Localized Surface Plasmon Resonance of Gold Nanorods. *ACS Nano* **2008**, *2*, 687–692.

13. Haes, A. J.; Hall, W. P.; Chang, L.; Klein, W. L.; Van Duyne, R. P. A Localized Surface Plasmon Resonance Biosensor: First Steps toward an Assay for Alzheimer's Disease. *Nano Lett.* **2004**, *4*, 1029–1034.

14. Nusz, G. J.; Marinakos, S. M.; Curry, A. C.; Dahlin, A.; Höök, F.; Wax, A.; Chilkoti, A. Label-free Plasmonic Detection of Biomolecular Binding by a Single Gold Nanorod. *Anal. Chem.* **2008**, *80*, 984–989.

15. Nehl, C. L.; Liao, H.; Hafner, J. H. Optical Properties of Star-Shaped Gold Nanoparticles. *Nano Lett.* **2006**, *6*, 683–688.

16. Hao, F.; Nehl, C. L.; Hafner, J. H.; Nordlander, P. Plasmon Resonances of a Gold Nanostar. *Nano Lett.* **2007**, *7*, 729–732.

17. Rodríguez-Lorenzo, L.; Álvarez-Puebla, R. A.; Pastoriza-Santos, I.; Mazzucco, S.; Odile, S.; Kociak, M.; Liz-Marzan, L. M.; García De Abajo, F. J. Zeptomol Detection Through Controlled Ultrasensitive Surface-Enhanced Raman Scattering. *J. Am. Chem. Soc.* **2009**, *131*, 4616–4618.

18. Hrelescu, C.; Sau, T. K.; Rogach, A. L.; Jäckel, F.; Feldmann, J. Single Gold Nanostars Enhance Raman Scattering. *Appl. Phys. Lett.* **2009**, *94*, 153113.

19. Chen, H.; Kou, X.; Yang, Z.; Ni, W.; Wang, J. Shape- and Size-Dependent Refractive Index Sensitivity of Gold Nanoparticles. *Langmuir* **2008**, *24*, 5233–5237.

20. Mock, J. J.; Smith, D. R.; Schultz, S. Local Refractive Index Dependence of Plasmon Resonance Spectra from Individual Nanoparticles. *Nano Lett.* **2003**, *3*, 485–491.

21. Raschke, G.; Feldmann, J.; Brogl, S.; Susha, A. S.; Rogach, A. L.; Klar, T. A.; Fieres, B.; Petkov, N.; Bein, T.; Nichtl, A.; *et al.* Gold Nanoshells Improve Single Nanoparticle Molecular Sensors. *Nano Lett.* **2004**, *4*, 1853–1857.

22. Lee, K.; El-Sayed, M. A. Gold and Silver Nanoparticles in Sensing and Imaging: Sensitivity of Plasmon Response to Size, Shape, and Metal Composition. *J. Phys. Chem. B* **2006**, *110*, 19220–5.

23. Nusz, G. J.; Curry, A. C.; Marinakos, S. M.; Wax, A.; Chilkoti, A. Rational Selection of Gold Nanorod Geometry for Label-free Plasmonic Biosensors. *ACS Nano* **2009**, *3*, 795–806.

24. Miller, M. M.; Lazarides, A. A. Sensitivity of Metal Nanoparticle Surface Plasmon Resonance to the Dielectric Environment. *J. Phys. Chem. B* **2005**, *105*, 21556–21565.